

# Generation of edge-preserved noise-added phase-only hologram

P. W. M. Tsang<sup>1,\*</sup>, Y. T. Chow<sup>1</sup>, and T.-C. Poon<sup>2</sup>

<sup>1</sup>Department of Electronic Engineering, City University of Hong Kong, Hong Kong SAR, China

<sup>2</sup>Bradley Department of Electrical and Computer Engineering, Virginia Tech, Blacksburg, 24061, USA

\*Corresponding author: eewmts@cityu.edu.hk

Received May 10, 2016; accepted August 19, 2016; posted online September 20, 2016

Noise addition is a simple but effective method for generating a phase-only hologram (POH) of an object. Briefly, the intensity image of an object is added with random phase noise and converted into a digital Fresnel hologram. Subsequently, the phase component of the hologram is retained as the POH. Although the method is fast and the visual quality of the reconstructed image is acceptable, the edges and lines patterns are heavily fragmented. In this Letter, we propose a method to overcome this problem. An experimental evaluation based on numerical and optical reconstructions reveals that a hologram generated by our proposed method is capable of preserving line patterns with favorable quality.

OCIS codes: 090.0090, 090.1995, 090.1760.

doi: 10.3788/COL201614.100901.

In light of the emergence of fast methods of computer-generated holography<sup>[1,2]</sup>, displaying a complex-valued digital hologram on an electronically accessible device has been a research topic of contemporary interest. Apart from academic interest, the enthusiasm for pursuing solutions for holographic display is also fueled by its potential in practical applications, such as compact projectors and head-up displays<sup>[3]</sup>. One of the biggest challenges encountered is how to display a complex-valued hologram with existing devices, commonly known as the spatial light modulators (SLMs), which are only capable of presenting either an amplitude image or a phase image. Reconstructing an image from a hologram with only one of the 2 components (amplitude or phase) will lead to heavy distortion. If only the phase component is retained, the smooth (shaded) regions of the reconstructed image will be heavily attenuated. Although it is possible to combine a pair of SLMs to display a complex-valued hologram<sup>[4]</sup>, the setup is complicated and expensive, which limits its usage in practical applications. Alternatively, the orthogonal components of the hologram can be displayed in non-overlapping partitions on a single SLM, and gratings and/or lenses are used to combine the optical waves of each section on the focused plane<sup>[5-8]</sup>. However, similar to the double SLM system, the optical setup of these methods is complicated, and the quality of the reconstructed image is degraded, as the effective display area is reduced by 2 times.

A more promising, but also time-consuming, solution is to generate a phase-only hologram (POH) based on the Gerchberg-Saxton (GS) algorithm<sup>[9]</sup> or the iterative Fresnel transform<sup>[10]</sup>. A faster approach has been suggested in Ref. [11] for converting a complex-valued hologram to a POH through error diffusion. However, due to the recursive nature of error diffusion, the computation time is too

lengthy for hologram generation at a video rate. So far, the fastest and simplest methods for generating POH are the random noise addition (RNA)<sup>[12]</sup> and the down-sampling (DS)<sup>[13-15]</sup> algorithms. With the noise addition method, random phase noise is added to the source image, while in the DS method, the image is converted into a sparse form. In both cases, when the processed image is converted into a complex-valued hologram, retaining the phase component alone will be sufficient to preserve the essential information of the hologram. Comparatively, the reconstructed image of the hologram obtained with DS is sparse (with regular patterns of empty holes) due to the removal of some pixels in the DS process, while that of the hologram derived with RNA is more solid in the smooth area, but the edge and line patterns are heavily fragmented.

In this Letter, we propose a method called “edge-preserved noise addition” (EPNA) to alleviate the above-mentioned problem of the RNA method. An experimental evaluation based on numerical and optical reconstructions reflects that a POH generated with our proposed method is capable of preserving favorable visual quality on both the smooth intensity regions and the line patterns.

For the sake of clarity, we would like to provide a brief concept of the RNA method that is reported in Ref. [12]. For simplicity of the explanation and demonstration of our proposed method, we have assumed that the source image  $I(x, y)$  is a two-dimensional (2-D) image that is parallel to, and at a distance  $z_o$  from, the hologram plane, as shown in Fig. 1. The RNA method can be divided into 2 stages. In stage 1, the source image is first added with random noise  $N(x, y) = e^{j\theta(x,y)}$  (where  $\theta(x, y) \in [0, 2\pi)$  is a random value with uniform distribution), and the result is a noise-added image  $I_N(x, y) = I(x, y)e^{j\theta(x,y)}$ . Subsequently, in stage 2, the noise-added image  $I_N(x, y) = I(x, y)e^{j\theta(x,y)}$  is converted into a complex-valued hologram, as

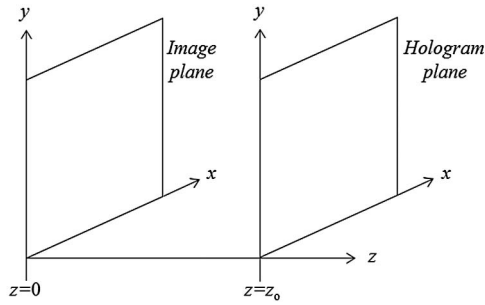


Fig. 1. Image and the hologram planes.

$$H(x, y) = I_N(x, y) * h(x, y; z_0), \quad (1)$$

where  $h(x, y; z_0) = \exp j(2\pi/\lambda\sqrt{x^2 + y^2 + z_0^2})$ , and  $\lambda$  is the wavelength of the optical beam.

Subsequently, the phase component of  $H(x, y)$  is retained as a POH  $H_P(x, y)$ . The addition of the random phase is similar to using a diffuser, which scatters the pixels of the source image into a more or less constant magnitude wavefront. As we shall show later, the reconstructed image of the RNA hologram is capable of preserving the smooth regions of the source image with reasonable quality, but the lines and edges will be fragmented due to the addition of the random noise.

In our proposed EPNA method, we avoid the degradation to the lines and edges by selectively adding the random noise to the smooth regions of the source image. Our proposed method can be divided into 3 stages, as illustrated in Fig. 2 and described as follows.

1st Stage: Image segmentation.

In the first stage, the difference between each pixel of the source image, and the weighted sum of its eight immediate neighbors, is computed as

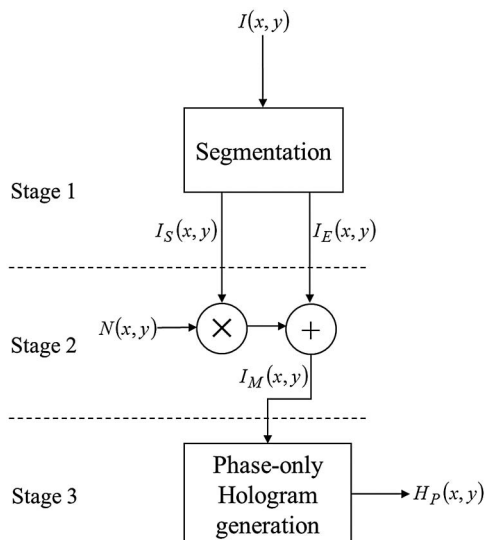


Fig. 2. Proposed method for generating the EPNA POH.

$$I_D(x, y) = I(x, y) - \frac{1}{8} \sum_{m=-1}^{m=1} \sum_{n=-1}^{n=1} I(x+m, y+n) |_{m \neq n}, \quad (2)$$

resulting in a high-pass filtered image  $I_D(x, y)$ . Pixels in the high-pass filtered image that exhibit large values represent rapid changes in intensities that are generally constituted by edges and line patterns. On this basis, an edge image  $I_E(x, y)$  is extracted from the source image as

$$I_E(x, y) = \begin{cases} I(x, y) & |I_D(x, y)| > \text{threshold} \\ 0 & \text{otherwise} \end{cases}, \quad (3)$$

where the threshold is a constant value. Our proposed method is not too sensitive to the threshold value. In general, a threshold value of  $(\frac{1}{32})^{\text{th}}$  of the maximum intensity of the image will generally lead to good discrimination between the smooth regions and the edge patterns in an image.

Next, a non-edge image  $I_S(x, y)$  is derived by removing all the pixels that correspond to the edge image  $I_E(x, y)$ , i.e.,

$$I_S(x, y) = I(x, y) - I_E(x, y). \quad (4)$$

2nd Stage: Noise addition.

Due to the removal of the edge image in Stage 1, the content of the non-edge image  $I_S(x, y)$  is generally smooth. As explained previously, the shaded regions will be severely distorted when an image is directly converted into a POH by simply discarding the magnitude component of the hologram. To alleviate this kind of degradation, random phase noise,  $N(x, y)$ , is added into the non-edge image, as given by

$$I_{NS}(x, y) = I_S(x, y) \times N(x, y). \quad (5)$$

Subsequently,  $I_E(x, y)$  and  $I_{NS}(x, y)$  are summed up to give a modified source image  $I_M(x, y)$ .

3rd Stage: Generation of POH.

In this stage, the modified source image is converted to a complex-valued hologram  $H(x, y)$  with Eq. (1). The phase component of  $H(x, y)$  is then retained as the POH.

The test image in Fig. 3, which is comprised of line patterns and smooth regions, is employed to illustrate



Fig. 3. Test image.

**Table 1.** Optical Settings for Generating the Digital Hologram

Wavelength $\lambda$	633 nm
Pixel size of hologram/object image	$8.1 \mu\text{m} \times 8.1 \mu\text{m}$
Size of hologram	$2048 \times 2048$
Size of object image	$512 \times 512$

our proposed method. To begin with, a complex-valued hologram that is parallel to and located at an axial distance of 0.3 m from the image is numerically generated based on the optical settings in Table 1. The numerical reconstructed image of the complex-valued hologram is shown in Fig. 4(a). Subsequently, we apply the RNA method and our proposed EPNA method to compute the POHs of the test image based on identical optical settings. The numerical reconstructed images of the 2 POHs are shown in Figs. 4(b) and 4(c), respectively. Compared with the reconstructed image of the complex-valued hologram, we observed that for the RNA hologram, the lines and edges of the reconstructed image are broken in many places (the vertical and the horizontal lines of the square enclosing the text characters), but they are preserved favorably in the EPNA hologram. The peak-signal-to-noise ratio (PSNR) (see Appendix) between the reconstructed images of the complex-valued hologram and the reconstructed images of the POHs obtained with the RNA method is 22.73 dB. The PSNR between the reconstructed images of the complex-valued hologram and the reconstructed images of the POHs obtained with our proposed method is 24.37 dB. It can be seen that the PSNR of the reconstructed image corresponding to the POH derived with our method is about 1.6 dB higher than that of the RNA hologram.

The optical reconstructed results of the RNA and the EPNA POHs are displayed on a  $1920 \times 1080$ ,  $8.1 \mu\text{m}$  Holoeye HEO1080 phase-only SLM with the optical setup given in Fig. 5. The SLM is directly illuminated with a

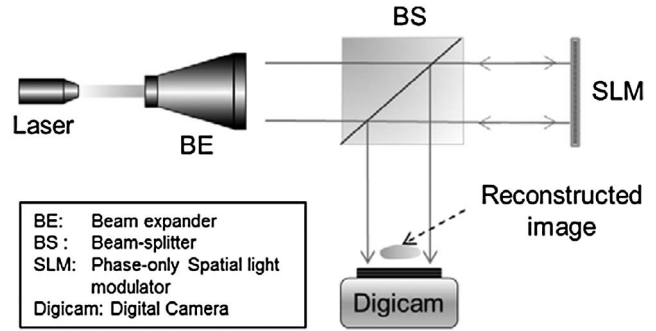


Fig. 5. Optical setup for displaying the POH.

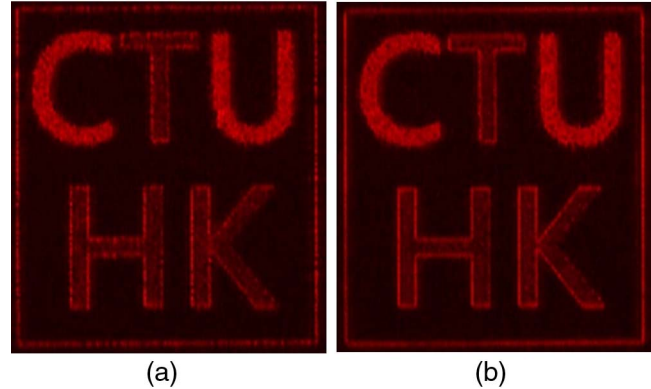


Fig. 6. (a) Optical reconstructed image of the POH of the test image, generated by the RNA method and (b) optical reconstructed image of the POH of the test image, generated by the proposed EPNA method.

plane wave that is derived from a 633 nm red semiconductor laser and a beam expander. The reconstructed image is reflected from a beam splitter and captured with a digital camera. The optical reconstructed images of the RNA and the EPNA POHs are shown in Figs. 6(a) and 6(b), respectively. We observed that the optical and numerical reconstructed images at the focused plane (0.3 m from the hologram) are similar, apart from some minor difference

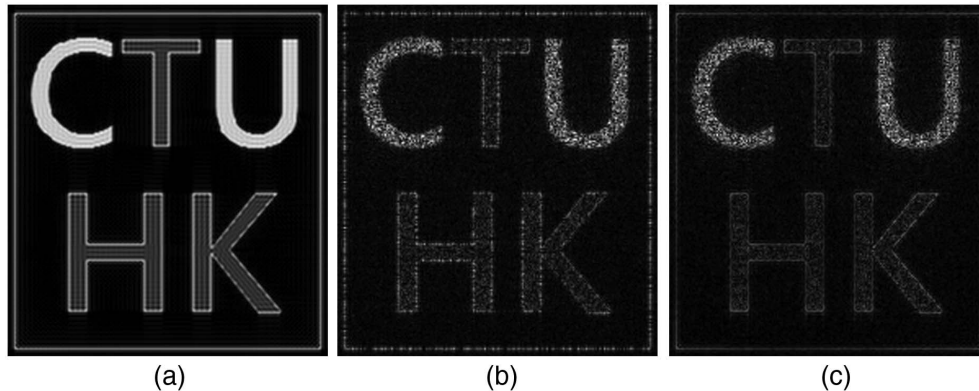


Fig. 4. (a) Numerical reconstructed image of the complex-valued hologram of the test image, (b) numerical reconstructed image of the POH of the test image, generated by the RNA method, and (c) numerical reconstructed image of the POH of the test image, generated by the proposed EPNA method.

that is caused by the imperfection of the optical display setup. Clearly, the lines and edges of the reconstructed image of the proposed EPNA hologram are preserved more favorably and are much less fragmented than those of the RNA hologram. The above qualitative and quantitative evaluations both demonstrated that the performance of our proposed method is superior to the RNA method. Having said that, we would also like to point out that the broken edges and boundaries of the reconstructed image of the RNA hologram also cast the impression of a sharper appearance, as compared with the EPNA hologram.

This Letter describes a non-iterative method for the fast generation of a POH. In our proposed method, a segmentation unit is employed to detect the non-edge (i.e., the smooth intensity) contents, in which random noise is added. The modified image is then converted into a complex-valued Fresnel hologram, and the phase component is retained as a POH. We have demonstrated, through numerical and optical reconstruction, that both the smooth regions and the edge/line patterns are preserved favorably in a POH generated with our proposed method.

### Appendix

The similarity between a pair of images  $f(x, y)$  and  $g(x, y)$ , both comprised of  $X$  columns and  $Y$  rows of pixels, can be reflected by the PSNR, as given by

$$\text{PSNR} = 10 \log_{10} \frac{\text{MAX}^2}{\sum_{x=0}^X \sum_{y=0}^Y [f(x, y) - g(x, y)]^2},$$

where MAX is the maximum intensity a pixel can reach. The unit of the PSNR is decibels (dB). A larger PSNR

value reflects a higher degree of similarity between a pair of images, and vice versa.

### References

1. J. Weng, T. Shimobaba, N. Okada, H. Nakayama, M. Oikawa, N. Masuda, and T. Ito, *Opt. Express* **20**, 4018 (2012).
2. P. W. M. Tsang, W. Cheung, T.-C. Poon, and C. Zhou, *Opt. Express* **19**, 15205 (2011).
3. J. Khan, C. Can, A. Greenaway, and I. Underwood, in *SID Mid-Europe Chapter Spring Meeting*, 82 (2013).
4. M. Makowski, A. Siemion, I. Ducin, K. Kakarenko, M. Sypek, A. Siemion, J. Suszek, D. Wojnowski, Z. Jaroszewicz, and A. Kolodziejczyk, *Chin. Opt. Lett.* **9**, 120008 (2011).
5. X. Li, Y. Wang, J. Liu, J. Jia, Y. Pan, and J. Xie, in *Digital Holography and 3-D Imaging*, OSA Technical Digest (OSA, 2013), paper DTh2A.3.
6. S. Reichelt, R. Häussler, G. Fütterer, N. Leister, H. Kato, N. Usukura, and Y. Kanbayashi, *Opt. Lett.* **37**, 1955 (2012).
7. H. Song, G. Sung, S. Choi, K. Won, H. Lee, and H. Kim, *Opt. Express* **20**, 29844 (2012).
8. J.-P. Liu, W. Hsieh, T.-C. Poon, and P. W. M. Tsang, *Appl. Opt.* **50**, H128 (2011).
9. P. Zhou, Y. Bi, M. Sun, H. Wang, F. Li, and Y. Qi, *Appl. Opt.* **53**, G209 (2014).
10. J. Yeom, J. Hong, J.-H. Jung, K. Hong, J.-H. Park, and B. Lee, *Chin. Opt. Lett.* **9**, 12009 (2011).
11. P. W. M. Tsang and T.-C. Poon, *Opt. Express* **21**, 23680 (2013).
12. I. Naydenova, Ed., *Advanced Holography—Metrology and Imaging*, Chap. 13 (InTech, 277, 2011).
13. P. W. M. Tsang, Y. T. Chow, T.-C. Poon, and J.-P. Liu, *Chin. Opt. Lett.* **14**, 010004 (2016).
14. P. W. M. Tsang, Y. T. Chow, and T.-C. Poon, *Chin. Opt. Lett.* **13**, 060901 (2015).
15. P. W. M. Tsang, Y. T. Chow, and T.-C. Poon, *Opt. Express* **22**, 25208 (2014).